The Journal of Neuroscience, June 1, 2000, 20(11):4145–4155

A-Type K^+ Current Mediated by the Kv4 Channel Regulates the Generation of Action Potential in Developing Cerebellar Granule Cells

Riichi Shibata,[1,3] Kensuke Nakahira,[1,4] Koji Shibasaki,[1,3] Yoshihiko Wakazono,[1] Keiji Imoto,[2,3] and Kazuhiro Ikenaka[1,3]

[1]Laboratory of Neural Information, [2]Laboratory of Humoral Information, Department of Informational Physiology, and [3]Department of Physiological Sciences, the Graduate University for Advanced Studies, National Institute for Physiological Sciences, and [4]Center for Bio-Environmental Research, National Institute for Basic Biology, Okazaki National Research Institutes, Okazaki, Aichi 444–8585, Japan

During neuronal differentiation and maturation, electrical excitability is essential for proper gene expression and the formation of synapses. The expression of ion channels is crucial for this process; in particular, voltage-gated K^+ channels function as the key determinants of membrane excitability. Previously, we reported that the A-type K^+ current (I_A) and Kv4.2 K^+ channel subunit expression increased in cultured cerebellar granule cells with time. To examine the correlation between ion currents and the action potential, in the present study, we measured developmental changes of action potentials in cultured granule cells using the whole-cell patch-clamp method. In addition to an observed increment of I_A, we found that the Na^+ current also increased during development. The increase in both currents was accompanied by a change in the membrane excitability from the nonspiking type to the repetitive firing type. Next, to elucidate whether Kv4.2 is responsible for the I_A and to assess the effect of Kv4 subunits on action potential waveform, we transfected a cDNA encoding a dominant-negative mutant Kv4.2 (Kv4.2dn) into cultured cells. Expression of Kv4.2dn resulted in the elimination of I_A in the granule cells. This result demonstrates that members of the Kv4 subfamily are responsible for the I_A in developing granule cells. Moreover, elimination of I_A resulted in shortening of latency before the first spike generation. In contrast, expression of wild-type Kv4.2 resulted in a delay in latency. This indicates that appearance of I_A is critically required for suppression of the excitability of granule cells during their maturation.

Key words: Kv4.2; A-type current; dominant-negative; transfection; action potential; fast spike latency; microexplant culture; whole-cell patch clamp

Transient inactivating A-type current (I_A) is the predominant K^+ current in many mature neurons (Rogawski et al., 1985; Rudy et al., 1988; Bardoni and Belluzzi, 1993; Keros and McBain, 1997; Fisher et al., 1998; Hoffman and Johnston, 1998; Martina et al., 1998; Kanold and Manis, 1999) that is initially activated at the subthreshold range of membrane potential and inactivated during depolarizing pulses of duration. Heterologous expression studies have demonstrated that channels containing the Kv1.4, Kv3.4, and Kv4 subunits give rise to A-type channels (Baldwin et al., 1991; Schroter et al., 1991; Serodio et al., 1994, 1996; Surmeier et al., 1996). In addition, inactivating, A-type-like channels can be formed when ancillary β1 subunits are coexpressed with subunits of the Kv1 family that normally display delayed rectifier properties (Rettig et al., 1994; Heinemann et al., 1996; Sewing et al., 1996). Recent lines of evidence suggest that Kv4 subunits are the major components of I_A in the CNS (Tsaur et al., 1997; Serodio and Rudy, 1998), and Kv4 channel transcripts are thought to govern the discharge patterns of action potentials (Song et al., 1998; Kanold and Manis, 1999).

Although the functional significance of I_A is well established in the adult CNS, the associated developmental behaviors remain to be elucidated. In the case of amphibian spinal cord neurons, the expression of voltage-gated K^+ channels determines the differentiation of neurons to regulate the action potential waveform (Spitzer, 1995). In mammalian neurons, however, it has been difficult to clarify the function of K^+ channels because of the complexities of functional K^+ channel subunits, such as their molecular diversity, heteromultimeric assembly, and lack of selective blockers.

We reported previously that the level of expression of I_A increased with the development of the granule cells in microexplant cultures from neonatal mouse cerebella (Wakazono et al., 1997). Furthermore, we have reported recently that Kv4.2 proteins are detected in the premigratory zone (PMZ) of the cerebellum in which granule cells complete final division and initiate maturation (Shibata et al., 1999). The expression of Kv4.2 was also detectable in microexplant cultures and increases with the duration of the culture period. A concomitant increment of Kv4.2 and I_A was observed, implying that Kv4.2 may affect developmental changes in the excitability of developing granule cells.

Received Dec. 6, 1999; revised Feb. 16, 2000; accepted Feb. 24, 2000.

This work was supported by Grant in Aid 07458207 for Scientific Research on Priority Areas on "Functional Development of Neural Circuit," Grant in Aid #09780748, Ministry of Education, Science, Sports, and Culture of Japan, and a grant from the Hoansha Foundation. We thank Dr. T. Yagi for providing the cDNA library, Dr. M. Okabe for providing the pCXegfp vector, and Dr. J. S. Trimmer for providing the Kv1.1/RBG4 and Kv3.1/pCMV vectors.

Correspondence should be addressed to Dr. Kensuke Nakahira, Laboratory of Neural Information, Department of Informational Physiology, National Institute for Physiological Sciences, Okazaki National Research Institutes, 38 Nishigonaka, Myodaiji, Okazaki, Aichi 444–8585, Japan. E-mail: nakahira@nips.ac.jp.

Dr. Wakazono's present address: Photon Medical Research Center, Hamamatsu University School of Medicine, Hamamatsu 431-3192 Japan.

In the present study, we first demonstrated that action potentials shift from firing single spikes to repetitive firing during development of the cultured granule cells. Subsequently, to assess the contribution of I_A to the discharge pattern of membrane potential, we have used the somatic gene transfer method to introduce dominant-negative and wild-type Kv4.2 cDNA into the cerebellar granule cells of microexplant cultures using the lipofection method. Our results clearly demonstrate that density and inactivation kinetics of I_A mediated by Kv4 subunits are the key determinants that regulate the generation of the first spike in developing granule cells.

MATERIALS AND METHODS

Mouse Kv4.2 expression constructs. To isolate the mouse Kv4.2 homolog (mKv4.2), a mouse brain cDNA library constructed from 6-week-old C57BL/6 mice was screened using a rat sequence as a probe (the cDNA library was kindly provided by Dr. T. Yagi, National Institute for Physiological Sciences, Okazaki, Japan). A clone, named pK8, contained the mKv4.2 coding region and approximately 1.5 kb 5′ and 2.5 kb 3′ untranslated regions. A 2.5 kb fragment containing the entire coding region was isolated by digesting with *Bst*PI and *Eco*RI and used in the construction of expression vectors.

pCR3.1E was constructed from pCR3.1 (Invitrogen, Carlsbad CA). pCR3.1E contains the *enhanced green fluorescence protein* (*egfp*) gene instead of the *neo* gene in pCR3.1 through the replacement of a *Bln*I-*Bln*I fragment with an *egfp* fragment from pCXegfp (kindly donated by Dr. M. Okabe, Osaka University, Osaka, Japan). The mKv4.2 expression vector mKv4.2/pCR3.1E contains the mKv4.2 coding region at the *Eco*RI site of the vector, so that expression is under the control of the cytomegalovirus-immediately early (CMV-IE) promoter.

A dominant-negative mutation of mKv4.2, referred to as mKv4.2dn in this manuscript, was constructed as follows. The sequence that spans from the N-terminal region to the second transmembrane domain of mKv4.2 was amplified by PCR with the following primers: K8dn-f, CCGTCGACGTGGATGCCTGTTGCT; and K8dn-r, CTTATTC-GAAACGGTAACGACT. The amplified fragment was cloned into pCR2.1 using the TA-cloning kit (Invitrogen). The nucleotide sequence was confirmed by sequencing. Then, a Flag-tag sequence (Sigma, St. Louis, MO) was added to the C terminus of the clone by inserting double-stranded synthetic oligonucleotides: M2-f, CGACTACAAG-GACGACGATGACAAGTAAGTCGACG; and M2-r, CGTCGACT-TACTTGTCATCGTCGTCCTTGTAGT. A 229 bp *Nru*I-*Xho*I fragment of the resultant clone, K8dnM2/pCR2.1, was used to replace the C-terminal region of wild-type mKv4.2.

Because the CMV-IE promoter strength in the expression plasmids was insufficient in cerebellar granule cells, we switched the promoter to the stronger artificial, CAG promoter. To do this, mKv4.2 and mKv4.2dn were inserted into pCXegfp by replacing the *egfp* gene with the channel gene to make K8/pCX and K8dnM2/pCX, respectively. To identify the cells transfected with these constructs, pCXegfp was always cotransfected.

Cell culture and transfection. Microexplant cultures were prepared as described previously (Shibata et al., 1999). Cerebella with midbrain and brainstem were removed from 2- or 3-d-old mice and quickly transferred to PBS. After separating the cerebellum, pia matter was removed carefully with fine forceps. Then, the central region of the cerebellum was cut into four pieces in the sagittal direction, and white matter and the deep nucleus were removed with scalpels. After transferring the pieces of gray matter into Basal Medium Eagle (BME), they were cut into 200–300 μm pieces with scalpels. They were then placed on poly-L-lysine–laminin-coated glass coverslips with the serum-free BME containing fatty acid-free BSA (1 mg/ml), insulin (10 μg/ml), transferrin (100 μg/ml), aprotinin (1 μg/ml), L-thyroxine (0.1 nM), Na-selenite (30 nM), and glucose (2.5 mg/ml), and maintained in a CO_2 incubator.

Human embryonic kidney 293 (HEK293) cells (CRL-1573; American Type Culture Collection, Manassas, VA) were grown in DMEM supplemented with 10% fetal bovine serum at 37°C in a 5% CO_2 humidified incubator. Chinese hamster ovary-K1 (CHO-K1) cells (JCRB9018) were grown in Ham's F12 medium with 10% fetal bovine serum at 37°C in a 5% CO_2 humidified incubator. Cells were split and plated at 30–40% confluency on coverslips in four-well plates before transfection. Expression of Kv1.1 or Kv3.1 in CHO-K1 cells was performed by transfection with Kv1.1/RBG4 or Kv3.1/pCMV (kindly donated by Dr. J. Trimmer, State University of New York).

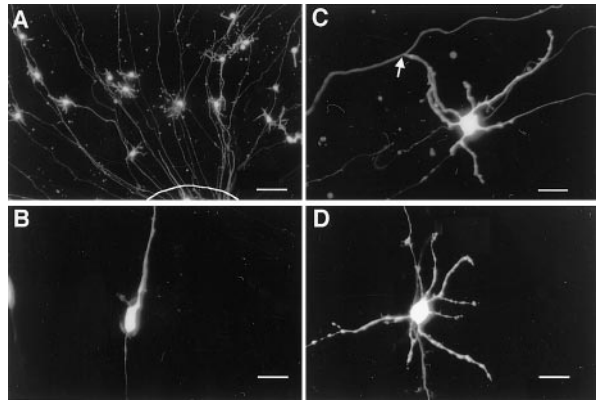

Figure 1. Expression of EGFP in microexplant cultures using the lipofection method. *A*, A lower magnification of EGFP-positive cells near an explant at 7 DIV. The border of the explant is indicated by a *line*. The EGFP expression vector was transfected at 4 DIV. Approximately 10 cells per explant were labeled with EGFP. Most positive cells had short dendrites and a pair of long processes extending radially to the explant. These cells were typical granule cells. *B*, Representative bipolar cell observed at 2 DIV. EGFP cDNA was transfected at 1 DIV. *C*, Typical T-shaped cell observed at 7 DIV. The *arrow* points to the T-junction. *D*, Many mature granule cells had dendrites but did not exhibit T-shape. Scale bars: *A*, 50 μm; *B–D*, 10 μm.

Twenty-four hours after plating, cells were transfected with plasmid DNA (0.2 μg/well) using LipofectAMINE plus (Life Technologies, Grand Island, NY). For microexplant culture cells, transfection was performed at 1 day *in vitro* (DIV) or 4 DIV. The first EGFP-positive cells were detectable at 12 hr after transfection, and ~10 cells per explant became EGFP-positive. Currents and action potential were recorded 3 d after the transfection.

Electrophysiology. Cells were thoroughly washed with the extracellular solution containing (in mM): 145 NaCl, 2.5 KCl, 2 $CaCl_2$, 1 $MgCl_2$, 5 HEPES, and 10 glucose, pH adjusted to 7.4 with NaOH. In the voltage-clamp experiments, we perfused the cells with an extracellular solution containing (in mM): 145 NaCl, 2.5 KCl, 2 $MnCl_2$, 1 $MgCl_2$, 5 HEPES, 10 glucose, and 0.001 tetrodotoxin (TTX), pH adjusted to 7.4 with NaOH, to block Na^+ channel currents, Ca^{2+} channel currents, and Ca^{2+}-activated K^+ currents. Recording pipettes were pulled from borosilicate glass tubing (Narishige, Tokyo, Japan) and heat-polished before use. Recordings were performed with patch pipettes that had 5–10 MΩ resistance when filled with the following solution (in mM): 140 potassium gluconate, 10 KCl, 2 $CaCl_2$, 1 $MgCl_2$, 0.5 EDTA, 5 HEPES, and 10 glucose, pH adjusted to 7.2 with KOH. Whole-cell patch-clamp recordings were performed at room temperature with a patch-clamp amplifier (Axopatch-1D; Axon Instruments, Foster City, CA). The recording was performed using a fluorescent microscope from cells that were labeled with EGFP to identify their morphology. Capacitative transients and series resistance (20–30 MΩ) were compensated in the whole-cell mode, and leakage currents were not subtracted. Cell capacitance and series resistance were read from the dials of the patch-clamp amplifier. Potentials were not corrected for liquid junction potential (−6 mV). Stable recordings could be obtained later than 3 min after breakthrough, which in these small cells should allow equilibration of the pipette content with the cytosol. In current-clamp mode, all compensations were set free. Membrane voltage and current were filtered at 2 or 10 kHz using a four-pole low-pass Bessel filter. Data acquisition and voltage control were performed with a computer-controlled interface using pClamp software version 5.5.1 (Axon Instruments). Curve fitting and statistical calculations were performed with Origin (Microcal, Northampton, MA).

I_A component was isolated using the prepulse protocol. This protocol is performed by subtracting the current evoked by a test pulse (+20 mV) after a 200 msec voltage step at −20 mV (prepulse) at which the A-type channels were fully inactivated, from the current evoked from a holding potential (−80 mV).

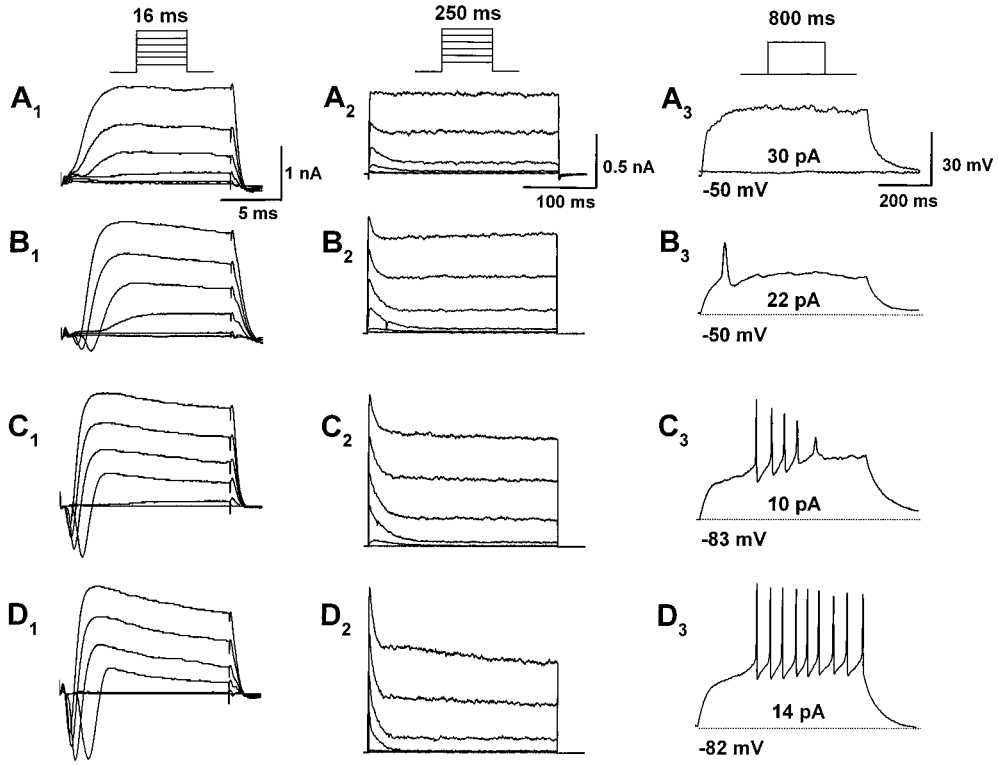

Figure 2. Developmental changes in membrane current and action potential in the granule cells. *A*, Representative whole-cell current (A_1 and A_2) and voltage response (A_3) recorded from a bipolar cell at 2 DIV. Records were obtained from the same cell. A_1, Cell was elicited with step depolarizations from a holding potential of −80 mV to a potential of between −60 and +40 mV with 20 mV increments for 16 msec in voltage-clamp mode to monitor fast inward currents (*inset*; the same protocol was applied in B_1, C_1, and D_1). Fast-rising inward currents were not evoked in bipolar cells. A_2, The same protocol as shown in A_1 was applied for 250 msec to monitor outward currents (this protocol was also applied in B_1, C_1, and D_1). A_3, A depolarizing current step of 30 pA for 800 msec did not evoke action potential from a holding potential of −50 mV. *B–D*, Representative whole-cell currents (B_1, B_2, C_1, C_2, D_1, and D_2) and voltage responses (B_3, C_3, and D_3) recorded from T-shaped cells at 4–7 DIV. Recordings in *B*, *C*, and *D* were obtained from the same cell. Fast-rising inward currents and fast-inactivating currents increased in T-shaped cells. B_3, C_3, D_3, A depolarizing current step of 22 (B_3), 10 (C_3), or 14 (D_3) pA was applied for 800 msec from a holding potential of −50 (B_3), −83 (C_3), or −82 (D_3) mV, respectively. In the T-shaped cells, three types of discharge patterns, single spike (B_3), rapidly adapting (C_3), and repetitive firing (D_3), were observed.

Data analysis. The program provides an estimate of current amplitude (I) as a function of time (t) according to the equation:

$$I(t)=A_0+A_1\exp(-t/t_1)$$

The solution to this equation determines the sum of noninactivating currents (A_0) and the amplitude (A_1) and time constants (t_1) that best fit the evoked current.

To analyze steady-state activation, we fit the currents to the following normalized Boltzmann equation:

$$I(V)=G_{max}(V-V_r)/\{1+\exp[-(V-V_{0.5})/k]\}$$

where I is the membrane current (in picoamperes) at the command voltage, V is the command voltage (in millivolts), V_r is the reversal potential for the K^+ current (estimated as −70 mV), G_{max} is the maximal conductance (in nanosiemans) [$G = I/(V - V_r)$], $V_{0.5}$ is the membrane potential for half-activation, and k is the slop factor.

To analyze steady-state inactivation, we fit the currents to the following normalized Boltzmann equation:

$$I(V)=I_{max}/\{1+\exp[-(V-V_{0.5})/k]\}$$

where I is the membrane current (in picoamperes) at the command voltage, and I_{max} is the maximal current (in picoamperes) to the step (20 mV) measured after a 200 msec control prepulse to −120 mV.

All data reported in this study are expressed as means ± SEM. Comparisons between groups were made using the Student's paired t test. Differences were considered to be significant when $p < 0.05$ ($^*p < 0.05$, $^{**}p < 0.01$, $^{***}p < 0.001$). Regression fit in Figure 3 was given by the least-squares equation.

RESULTS

Developmental change of electrophysiological properties

Granule cells in the microexplant culture initially extend a pair of long axons and then change morphology from bipolar to T-shaped (Nagata and Nakatsuji, 1990; Wakazono et al., 1997). To record their morphology and electrophysiological responses simultaneously, we previously used Lucifer yellow, which had been added into the patch-pipette solution to label the cells. However, cell shape recognition was impossible before pipette attachment to the cells. Thus, in this study, cells were labeled with EGFP, which was expressed from an expression vector transfected at 1 or 4 DIV. Figure 1*A* shows EGFP-positive cells near the explant. Approximately 10 cells per explant were labeled and became detectable 12 hr after transfection. The labeling experiments showed that bipolar cells (Fig. 1*B*) were observed mainly at 2–3 DIV, but few cells were detected in later stages. On the contrary, T-shaped cells (Fig. 1*C*) started to appear at 4 DIV, and the number increased thereafter. Sequential observation of a single labeled granule cell confirmed that they change their morphology with development *in vitro*. The cells that did not exhibit clear T-shapes but possessed several dendrites along with the long thin axons were present predominantly in later periods of culture (Fig. 1*D*). We speculated that the absence of glial cells, which were

necessary for neural locomotion, prevented the efficient movement of cell bodies perpendicular to the parallel fibers. Therefore, we also categorized such cells as mature T-shaped cells. We found no differences in electrophysiological responses between typical T-shaped cells and incomplete T-shaped cells.

To demonstrate the developmental changes in membrane properties, we compared bipolar cells at 2 DIV and T-shaped cells at 7 DIV. The membrane capacitance, resting membrane potential (RMP), and input resistance were measured. Capacitance increased ~1.5-fold from bipolar cells (3.7 ± 1.2 pF, $n = 10$) to T-shaped cells (5.8 ± 0.3 pF, $n = 12$). Similar results were reported using dissociated granule cells (Gorter et al., 1995), whereas the opposite was reported using cerebellar slices in which the capacitance of granule cells did not increase during development (D'Angelo et al., 1997; Rossi et al., 1998). The RMP was measured shortly after establishing whole-cell recording mode. The bipolar cells had relatively depolarized RMP (−41.4 ± 3.4 mV, $n = 7$), and the T-shaped cells had more negative values (−65.8 ± 2.6 mV, $n = 26$). This result indicates that the RMP shifted to negative potential during development. The input resistance was calculated using Ohm's law from the voltage response to a hyperpolarizing current injection. To avoid distortion by activation of voltage-dependent conductance, a small current (−50 pA) was used. The input resistance was high (7.2 ± 0.2 GΩ, $n = 6$) in bipolar cells but low (2.3 ± 0.1 GΩ, $n = 6$) in T-shaped cells. The decrease in input resistance during development is considered to reflect an increase in functional ion channels that were active around RMP. The negative shift of RMP and decrease in input resistance were consistent with both cultured (Ramoa and McCormick, 1994) and *in vivo* (D'Angelo et al., 1997; Rossi et al., 1998) granule cells.

Action potential and voltage-dependent currents

Next, we investigated developmental changes in excitability using whole-cell voltage-clamp and current-clamp configurations. Responses were recorded from bipolar cells at 2 DIV (Fig. 2*A*) and T-shaped cells at 4–6 DIV (Fig. 2*B–D*). We did not use any channel blockers to record inward current and outward K^+ current along with action potential.

Figure $2A_1$–A_3 shows typical recordings from a bipolar cell. Depolarizing potentials were applied to the cells for 16 (Fig. $2A_1$) or 250 (Fig. $2A_2$) msec to record fast inward currents and net outward currents, respectively. In bipolar cells, no inward current was observed at any voltage pulse applied to the membrane. As reported previously by Wakazono et al. (1997), slowly inactivating delayed rectifier currents were present predominantly, and a small amount of fast inactivating I_A was observed. When depolarizing currents were injected, no action potential was generated (Fig. $2A_3$).

The T-shaped granule cells exhibited four distinct discharge patterns in response to depolarizing current injection under the current-clamp mode (Fig. 2*B–D*). Among 26 cells we recorded in this experiment, 23% (6 of 26) of the cells exhibited single action potential (single-type) (Fig. $2B_3$). Fifty percent (13 of 26) of the cells exhibited rapid adapting repetitive firing (adapting-type) (Fig. $2C_3$), and 23% (6 of 26) of the cells exhibited nonattenuating repetitive firing (repetitive-type) (Fig. $2D_3$). Only one T-shaped cell did not produce action potential, even after injection of a large current (silent cell) (data not shown). The silent cell was observed at 4 DIV of microexplant culture, and the single- and adapting-type cells appeared at 4–5 DIV. The repetitive-type firing emerged after 6 DIV. These results suggest the occurrence of a development-related shift in the different response patterns. Furthermore, the resting membrane potentials for each of the cell types were −46.6 ± 4.9 (mean ± SEM, single-type cells; $n = 6$), −66.3 ± 4.1 (adapting-type cells; $n = 13$), and −78.0 ± 2.2 mV (repetitive-type cells; $n = 6$), respectively. These data also support the idea that action potential changed from single to repetitive during the development of granule cells.

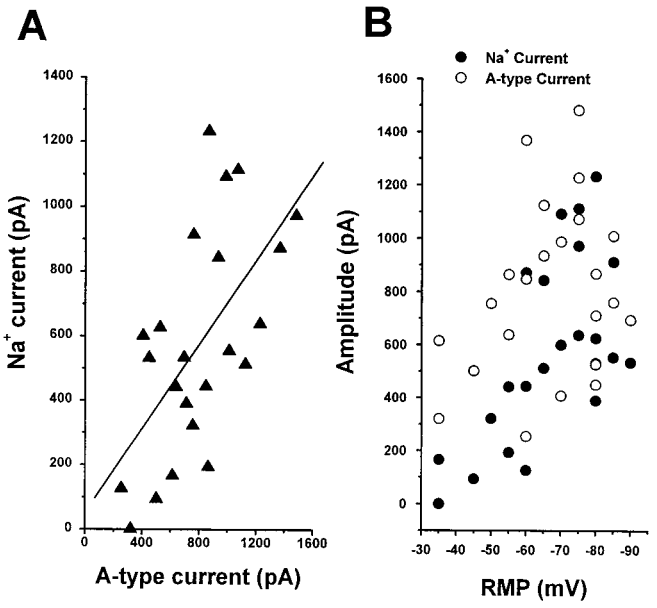

Figure 3. A-Type currents and Na^+ currents increased over a similar time course. *A*, The amplitude Na^+ current was plotted as a function of A-type current recorded from the same cell. These currents were recorded from a mix of bipolar and T-shaped cells. A-Type current was isolated by the prepulse protocol, and its peak amplitude was measured. The relationship between the A-type current and the Na^+ current was fitted by the least-squares method (*solid line*; $r = 0.65$). *B*, The size of the Na^+ current (*filled circles*) and the A-type current (*open circles*) was plotted as a function of RMP. Note that the increase in amplitude of both currents correlated with the depth of the RMP.

To determine whether the change of firing pattern is attributable to the appearance of specific membrane conductance, ion currents were compared. In the single-type cells, small inward currents were observed (Fig. $2B_1$). The amplitude of the inward currents was increased in the adapting-type cells (Fig. $2C_1$) and further increased in the repetitive-type cells (Fig. $2D_1$). This indicates that the level of inward currents is accompanied by the onset of repetitive firing. Both inward currents and action potential were completely eliminated by the application of 1 μM TTX (data not shown). Thus, the action potential of the cells is critically dependent on the activation of TTX-sensitive Na^+ channels. Figure 2, B_2, C_2, and D_2, shows the developmental changes of outward currents in T-shaped cells. The amplitude of fast-inactivating current components, as well as the inward current, increased.

Because the developmental changes in the amplitude of Na^+ and the I_A were very similar, we plotted Na^+ currents as a function of I_A (Fig. 3). The I_A was isolated by a prepulse protocol. The size of Na^+ currents was in proportion to that of I_A ($I_{Na} = 51 + 0.65 \cdot I_A$; $r = 0.61$) (Fig. 3*A*). Furthermore, these two currents also exhibited correlation with the RMP. As RMP became more negative, the amplitudes of Na^+ and I_A became larger (Fig. 3*B*). These data indicate that increments of Na^+ current and I_A are accompanied by maturation of granule cells.

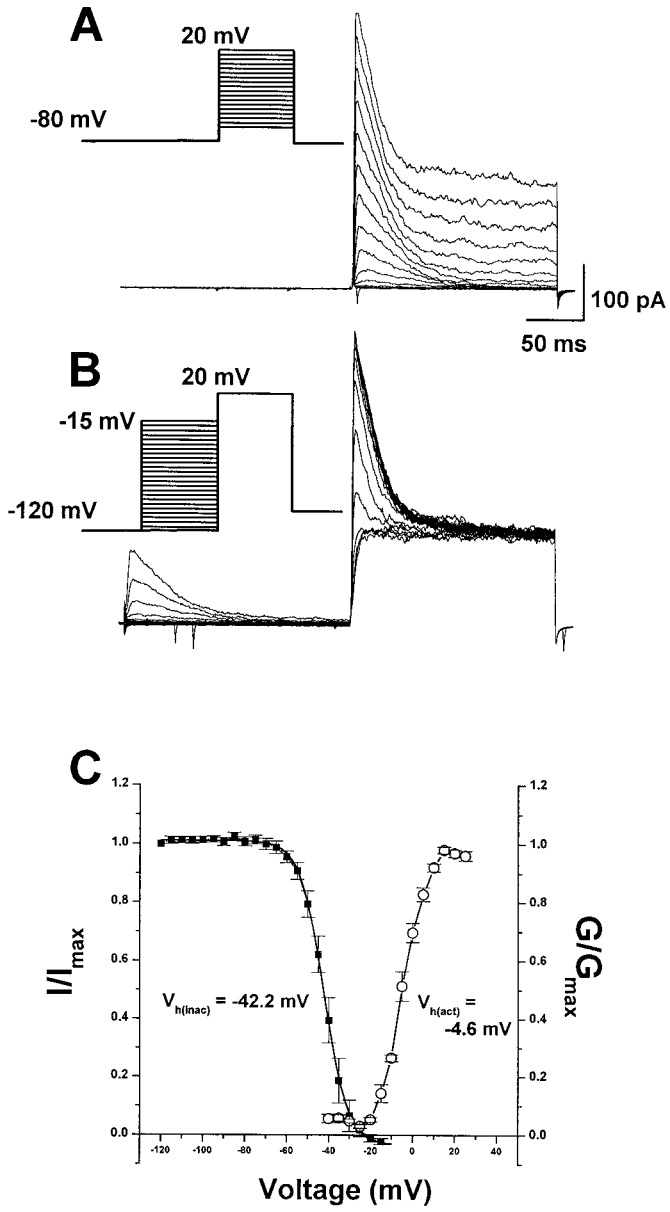

Figure 4. Voltage dependence of activation and inactivation of transient current in the granule cells. *A*, Superimposed current traces evoked by depolarizing steps to potentials between −60 and +20 mV with 5 mV increment after −80 mV. *B*, Superimposed current traces evoked by test depolarization to +20 mV after 200 msec prepulse to potentials between −120 and −15 mV with 5 mV increment. *C*, Plot of normalized peak current as a function of conditioning voltage. Boltzmann functions with half-activation voltage of −4.6 mV and half-inactivation voltage of −42.2 mV. Spontaneous inward spikes occasionally remained after blockade of spontaneous activity by TTX and Ca^{2+} channel blocker.

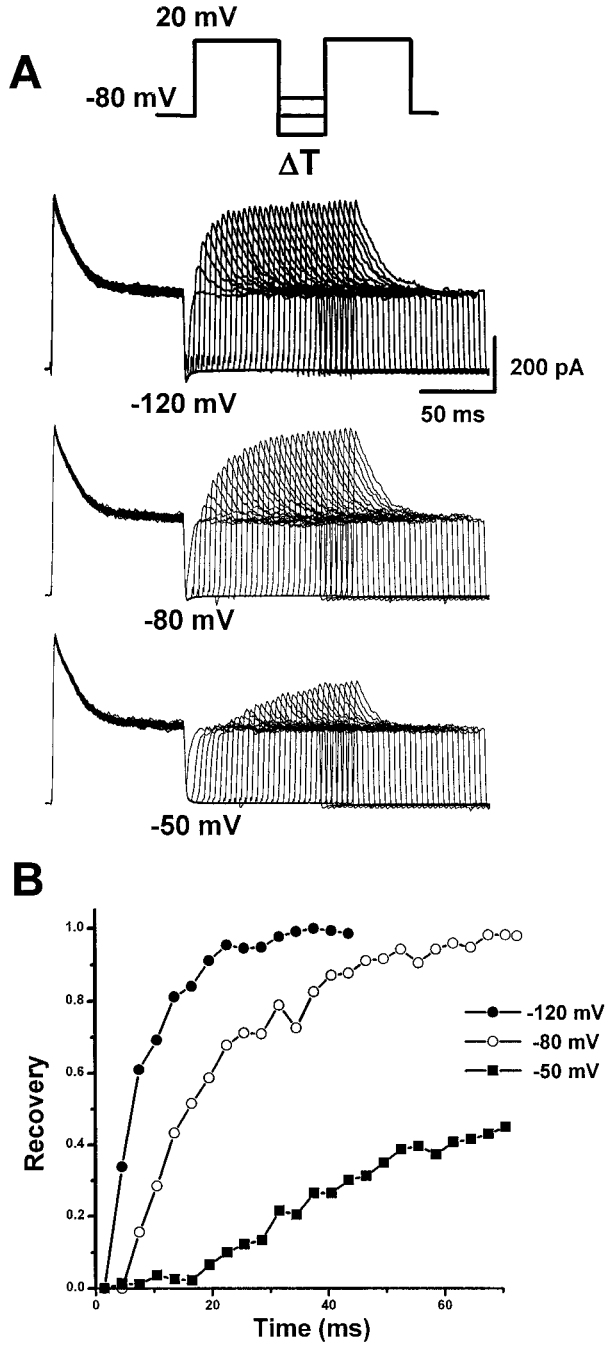

Figure 5. Recovery from inactivation of A-type currents. *A*, Inactivation recovery was examined by inactivating the A-type current and then stepping to −120, −80, or −50 mV for increasing before a test step to 20 mV. The voltage protocol is shown above the current traces. Current traces recovered from −120 (*top traces*), −80 (*middle traces*), and −50 (*bottom traces*) mV are shown. *B*, Plots of peak current as a function of prepulse duration at −120 (*filled circles*), −80 (*open circles*), and −50 (*filled squares*) mV. Data were fitted with a single exponential with time constants of 6.6 (at −120 mV), 15.5 (at −80 mV), and 41.4 (at −50 mV) msec, respectively.

Properties of I_A in granule cells

We characterized the voltage dependency of activation and inactivation of I_A in the granule cells. The voltage dependence of activation was studied by stepping the membrane voltage of the cells to potentials between −60 and +20 mV with 5 mV increments (Fig. 4*A*). The voltage dependence of inactivation was assessed by measuring the peak amplitude of current responses evoked by a 20 mV test pulse, after a 200 msec prepulse to conditioning voltages between −120 and −15 mV with 5 mV intervals (Fig. 4*B*). The mean activation of I_A is plotted as normalized conductance as a function of test voltage in Figure 4*C*. Fitting these data to the Boltzmann equation indicated the midpoints of activation (Vh_{act} of −4.6 mV) and inactivation (Vh_{inac} of −42.2 mV) and the slope factors (k_{act} of 5.0 mV and k_{inac} of 5.7 mV). These values are consistent with the previous report by Wakazono et al. (1997).

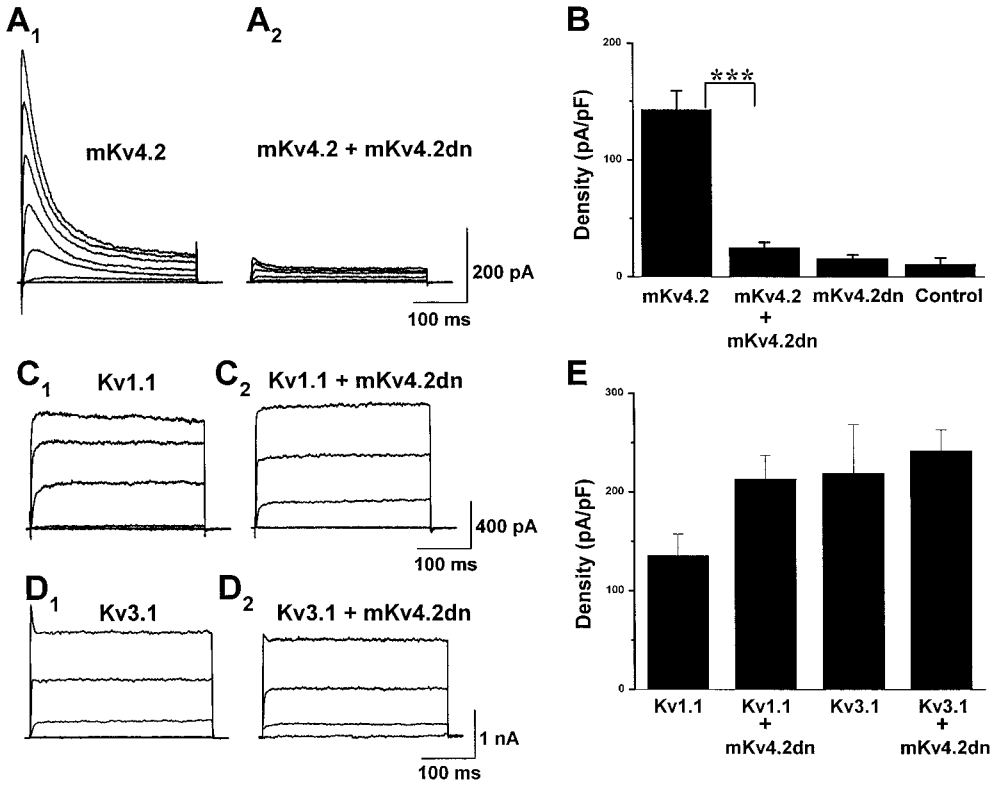

Figure 6. mKv4.2dn suppressed the mKv4.2 current in transiently transfected HEK293 cells. A_1, Wild-type mKv4.2 current was obtained when mKv4.2 and pCR3.1 vectors were cotransfected into HEK293 cells. Cells were held at −80 mV and then stepped to test potentials ranging from −60 to +40 mV (in 20 mV increments) for 250 msec. A_2, Wild-type mKv4.2 current was functionally eliminated when mKv4.2 and Kv4.2dn were cotransfected. Currents were evoked as described in A_1. *B*, Mean amplitude of peak currents at a +40 mV test pulse in HEK293 cells expressed with mKv4.2, mKv4.2 plus mKv4.2dn, mKv4.2dn, and pCR3.1E (mean ± SEM). The amplitude of the endogenous current expressed in HEK293 cells was measured from cells transfected with pCR3.1E. mKv4.2dn did not produce a functional current. The differences between mKv4.2 and mKv4.2 plus mKv4.2dn are statistically significant (Student's *t* test; $^{***}p < 0.001$). *C*, *D*, Kv1.1 current (C_1) or Kv3.1 current (D_1) was obtained when Kv3.1 were cotransfected into CHO-K1 cells. Cells were held at −80 mV and then stepped to test potentials ranging from −60 to +40 mV (in 20 mV increments) for 250 msec. Neither Kv1.1 current (C_2) nor Kv3.1 current (D_2) was suppressed by cotransfection with mKv4.2dn. *E*, Mean amplitude of peak currents at a +40 mV test pulse in CHO-K1 cells expressed with Kv1.1, Kv1.1 plus mKv4.2dn, Kv3.1, and Kv3.1 plus mKv4.2dn (mean ± SEM).

We then examined the recovery rate of I_A from inactivation (Fig. 5). A depolarizing voltage step was applied to fully inactivate the A-type channels, followed by a hyperpolarizing step of variable length to remove inactivation (the protocol is shown in Fig. 5*A*). The I_A took more than 40 msec to fully recover from inactivation at −120 mV, and the value of τ (recovery time constant) was 6.6 msec at −120 mV, 15.5 msec at −80 mV, and 41.4 msec at −50 mV (Fig. 5*B*).

The effect of dominant-negative mKv4.2 in HEK293 cells

Several studies have revealed the contribution of the I_A to discharge pattern based on pharmacological experiments (Cull-Candy et al., 1989; Bardoni and Belluzzi, 1993; D'Angelo et al., 1998). However, assessment of the specific role of I_A in these studies is difficult because of the loose selectivity of channel blockers. To identify the molecule carrying the I_A and its specific function in the regulation of action potential, we used dominant-negative constructs of mKv4.2. Johns et al. (1997) reported that a Kv4.2 dominant-negative construct, which had been truncated after the first transmembrane segment, suppressed currents encoded by Kv4 family genes. In the present experiment, we used a similar strategy. The mKv4.2 cDNA was cleaved at a position in the second intracellular loop, so that the resultant cDNA contained two transmembrane domains (mKv4.2dn).

To evaluate the efficiency of the dominant-negative effect of mKv4.2dn on mKv4.2-mediated current, the channel constructs were expressed in HEK293 (Fig. 6). This cell line expresses only a low level of voltage-gated K^+ channels and is therefore suitable for the analysis of channel activity introduced by gene transfer.

When the cells were transfected with wild-type mKv4.2, they expressed a fast-inactivating outward current with an inactivation rate of 20–30 msec at 20 mV depolarizing stimulation. The amplitude of mKv4.2 currents was 713.9 ± 80.5 pA/pF ($n = 5$) at +40 mV (Fig. 6A_1). The inactivation rate was similar to that reported previously using a *Xenopus* oocyte expression system (Serodio et al., 1994, 1996). To assess the effect of mKv4.2dn on mKv4.2 currents, they were cotransfected at a 1:1 molar ratio. The amplitude of emerging currents was reduced significantly (125.0 ± 22.5 pA/pF, $n = 8$) (Fig. 6A_2). The dominant-negative construct itself exhibited no significant current (77.0 ± 16.0 pA/pF, $n = 5$). To examine the specificity of mKv4.2dn, it was tested with Kv1.1 or Kv3.1 using CHO-K1 cells. Mean amplitudes of peak currents were compared in Figure 6*B*. Neither Kv1.1 (135.7 ± 21.4 pA/pF in Kv1.1 transfected cells, and 213.2 ± 23.8 pF/pA in Kv1.1 and mKv4.2dn transfected cells) (Fig. 6*C*) nor

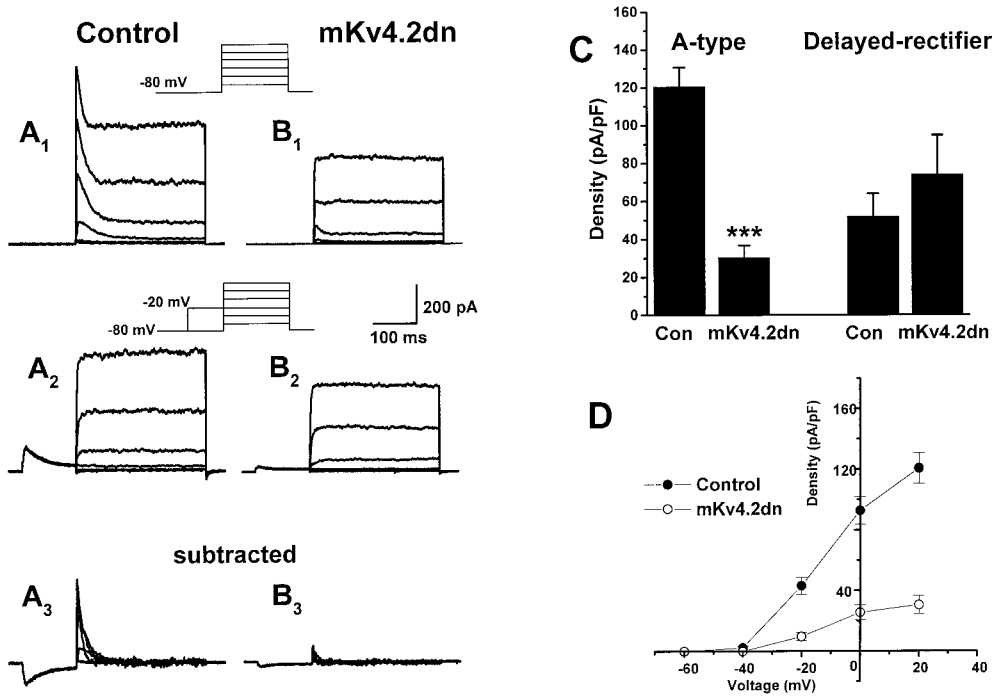

Figure 7. Expression of mKv4.2dn suppressed the A-type current of cerebellar granule cells. A_1, Cerebellar granule cells transfected with EGFP in the microexplant culture exhibited a large transient and maintained outward current by a series of depolarizing pulses of −60 to +40 mV. A_2, The transient component of the current can be inactivated with a prepulse to −20 mV. A_3, Isolated A-type current was obtained by subtracting A_2 from A_1. B_1–B_3, Cotransfection of mKv4.2dn and EGFP results in a marked suppression of the transient component without affecting the maintained component of outward currents. *C*, Quantitative analysis indicated the suppression of A-type current and no effect on delayed rectifier current in the peak density evoked at 20 mV. Mean ± SEM is displayed. $^{***}p < 0.001$ versus control cells. *D*, Voltage–current density relationship for A-type currents recorded from control cells (*filled circles*) and mKv4.2dn-transfected cells (*open circles*). Mean ± SEM is displayed.

Kv3.1 (219.0 ± 49.2 pA/pF in Kv3.1 transfected cells, and 241.9 ± 20.8 pA/pF in Kv3.1 and mKv4.2dn transfected cells) (Fig. 6*D*) was suppressed by the expression of mKv4.2dn, indicating that the effect of mKv4.2dn is specific to Kv4 (Fig. 6*E*).

The effect of mKv4.2 and mKv4.2dn in granule cells

We introduced mKv4.2dn into granule cells in the microexplant culture. Figure 7, *A* and *B*, shows typical examples of current trace recorded from a control cell and an mKv4.2dn-transfected cell. Separation of the transient and sustained currents was performed by the prepulse protocol (Fig. 7A_2,B_2). Isolated I_A are shown in Figure 7, A_3 and B_3.

In the control cells that were transfected with pCXegfp alone, the current density of isolated I_A was 120.6 ± 10.1 pA/pF at +20 mV ($n = 33$). On the other hand, in mKv4.2dn-transfected cells, it was drastically decreased to 30.5 ± 6.3 pA/pF ($n = 20$) (Fig. 7, compare A_3 and B_3; Fig. 7*C*). This effect of mKv4.2dn on K^+ currents was specific to I_A, because the delayed rectifier currents were not suppressed (52.0 ± 11.9 pA/pF in control cells, $n = 33$; 74.1 ± 20.5 pA/pF in mKv4.2dn-transfected cells, $n = 20$) (Fig. 7*C*). Figure 7*D* shows that mKv4.2dn suppresses I_A at all voltages from −60 to 40 mV. This result indicated that I_A observed in developing granule cells were carried by Kv4 (shal) family K^+ channels.

Next, we examined the effect of wild-type mKv4.2 expression in granule cells (Fig. 8). Figure 8*A* shows a representative current evoked by 20 mV of depolarizing voltage in a control cell and a mKv4.2-transfected cell. Transfection of mKv4.2 resulted in an increase in rate of inactivation. As shown in Figure 8*B*, the inactivation time constant of I_A decreased as depolarizing voltage increased in both control and mKv4.2-transfected cells, but the value recorded from mKv4.2-transfected cells was always approximately threefold larger than that of control cells. This value was similar to that obtained from transfected HEK293 cells. The density of I_A and voltage dependency of activation were not altered (Fig. 8*C*).

The effect of mKv4.2 and mKv4.2dn on membrane excitability

In mature T-shaped cells at 7 DIV, rapidly adapting and repetitive-type action potentials were recorded from both mKv4.2dn- and mKv4.2-transfected cells. This indicated that the ability to generate action potential developed normally, even when the exogenous genes were introduced. It is reported that the application of 4-AP, a blocker of I_A, altered the amplitude of afterhyperpolarization (AHP) and frequency of repetitive firing (D'Angelo et al., 1998). Therefore, we examined the properties of action potentials.

Figure 9*A* shows the action potentials recorded from control cells (A_1), mKv4.2dn-transfected cells (A_2), and mKv4.2-transfected cells (A_3). These traces clearly demonstrate that latency from the starting point of current injection to the peak of the first action potential [fast spike latency (FSL)] was different among these cells. FSL was shorter in mKv4.2dn-transfected cells (Fig. 9A_2) compared with the control cells, even when the injected current was smaller in mKv4.2dn-transfected cells (10 pA in nKv4.2dn, and 14 pA in control cells) (Fig. 9A_1). On the contrary, FSL was longer in mKv4.2-transfected cells (Fig. 9A_3), even when the injected current was larger (30 pA). In Figure 9*B*, mean FSL was plotted against the amount of injected current. The curve

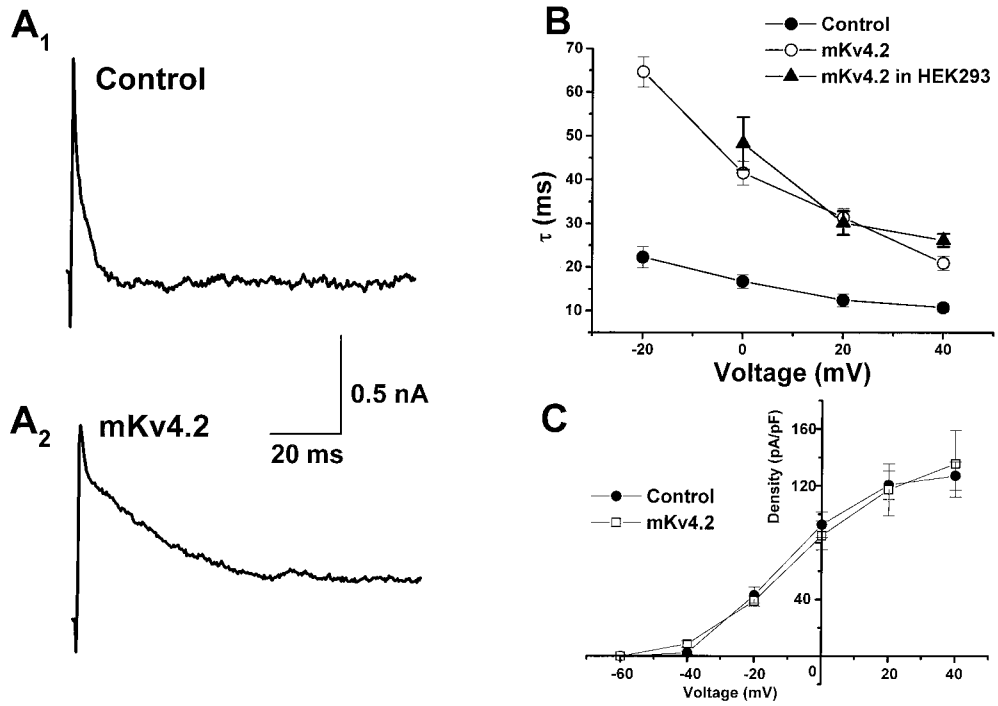

Figure 8. Expression of mKv4.2 altered the inactivation time constant of A-type currents in the cerebellar granule cells. *A*, Representative current recorded from a granule cell transfected with EGFP alone (A_1) and with EGFP plus mKv4.2 (A_2). Because the transfection of 0.2 μg/well mKv4.2 DNA caused serious damage to the granule cells (see Discussion), the amount of DNA for transfection was reduced to 0.05 μg/well. A depolarizing pulse to +20 mV from a holding potential of −80 mV was given. *B*, Time constant of inactivation as a function of voltage in control cells (*filled circles*) and mKv4.2-transfected cells (*open circles*). Time constant of inactivation of the mKv4.2 current in HEK293 cells (*filled triangles*) is also plotted. Mean ± SEM is displayed. *C*, Voltage–current density relationship for A-type currents recorded from control cells (*filled circles*) and mKv4.2-transfected cells (*open circles*). Mean ± SEM is displayed.

shifted to the left by the transfection of mKv4.2dn and shifted to the right by transfection of mKv4.2, indicating that I_A suppressed the generation of the first spike in developing granule cells. We also found that the FSL in control and mKv4.2-transfected cells became shorter to the level of mKv4.2dn-transfected cells when the membrane potential was preheld at −50 mV at which the A-type channels were inactivated (data not shown).

The minimum current required for generating action potential (Fig. 10*A*) and the amplitude of the first action potential (Fig. 10*B*) were also affected by alteration of I_A. The minimum injected current was 1.8 times smaller in mKV4.2dn-transfected cells and 2.2 times larger in wild-type mKV4.2-transfected cells. The amplitude of the first action potential was larger in mKv4.2dn-transfected cells (52.4 ± 2.6 mV, $n = 9$) and smaller in mKv4.2-transfected cells (37.2 ± 3.4 mV, $n = 4$) compared with the control cells (45.5 ± 1.4 mV, $n = 12$) (Fig. 10*B*).

In contrast to the parameters shown above, mKv4.2dn did not affect the depth of afterhyperpolarization (Fig. 10*C*). The inconsistency of this result with the effect of 4-AP on action potential is probably attributable to the blocking of other components of ion currents by 4-AP, such as delayed rectifier currents and Ca^{2+}-activated K^+ currents (Yeh et al., 1976; Thompson, 1982; Arhem and Johansson, 1989; Kehl, 1990; Davies et al., 1991; Choquet and Korn, 1992; Campbell et al., 1993; Castle and Slawsky, 1993). The threshold of action potential and RMP were also unaffected by the expression of mKv4.2 or mKv4.2dn (Fig. 10, *D* and *E*, respectively).

These results suggest that the specific role of Kv4 family channels on developing granule neurons is to suppress excitability by inhibiting the generation of the first spike.

DISCUSSION

Molecular identity and the role of the I_A

In the present study, we have demonstrated that the I_A in developing cerebellar granule cells of microexplant cultures was functionally eliminated by the dominant-negative mutant of mKv4.2 (Fig. 7). Although the voltage could not be clamped adequately in the long axonal and dendritic arbors of the granule cells, space-clamp error in the neurites did not affect the currents mediated by the Kv4 channel, because Kv4.2 proteins were localized to the cell body in this culture system, as we reported previously (Shibata et al., 1999). This result directly demonstrates that members of Kv4 α-subunits are responsible for the I_A. In adult cerebellar granule cells, Kv4.3, but not Kv4.1, expression was also reported (Serodio and Rudy, 1998). Thus, the probability that Kv4.2 and Kv4.3 form heteromultimeric complexes to conduct I_A cannot be ruled out. We showed previously that the expression patterns of Kv4.2 mRNA and protein correlated with the appearance of the I_A (Shibata et al., 1999), suggesting that this subunit is the major component of the A-type channels in the granule cells.

In addition, to provide a direct link between I_A and the Kv4 subfamily in developing granule cells, we demonstrated that, when functional Kv4 channels are eliminated, the latency to the first spike and the minimum injected current for spike generation greatly decreased (Figs. 9, 10). The effect of dominant-negative channels was restricted to the above phenomenon because other parameters, such as afterhyperpolarization, threshold, and RMP, did not change significantly. This finding revealed that the role of I_A is to control first spike latency without affecting the other parameters.

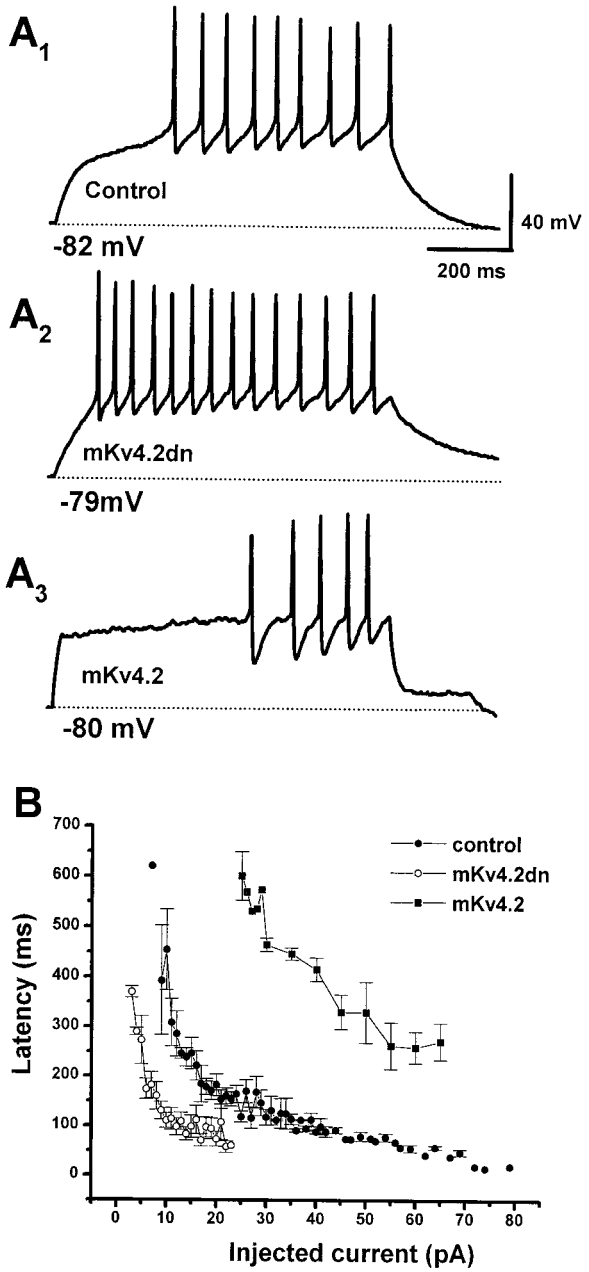

Figure 9. Effect of elimination or prolonged inactivation kinetics of A-type current on the latency to the first spike. *A*, Discharge pattern of EGPF-transfected cells (A_1, *Control*), mKv4.2dn plus EGFP-transfected cells (A_2), and mKv4.2 plus EGFP-transfected cells (A_3). The cells were held at or near −80 mV and injected with a current of 14 (A_1), 10 (A_2), or 30 (A_3) pA for 800 msec. *B*, The latency to the first spike was plotted as a function of amplitude of injected currents (mean ± SEM; $n = 6$ for control cells, $n = 4$ for mKv4.2dn-transfected cells, and $n = 5$ for mKv4.2-transfected cells). The FSL recorded from mKv4.2dn-transfected cells is shorter and the FSL from mKv4.2-transfected cells is longer compared with the FSL from control cells.

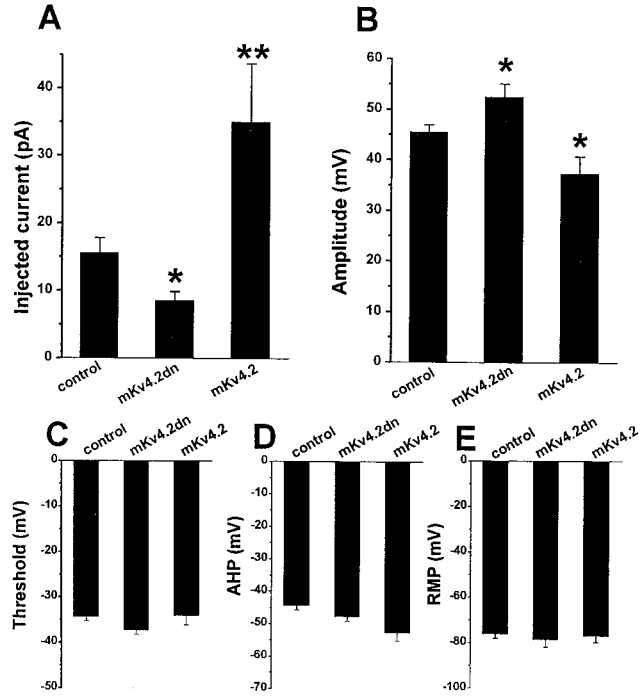

Figure 10. Effects of mKv4.2dn or mKv4.2dn expression on the physiology of granule cells. *A*, Minimum amplitude of injected current required for generating spikes. The data indicate that the minimum amplitude of injection was reduced in mKv4.2dn-transfected cells and increased in mKv4.2-transfected cells compared with control cells. Mean ± SEM. The differences between control cells ($n = 12$) and mKv4.2dn-transfected cells ($n = 9$, $^*p < 0.05$), or between control cells and mKv4.2-transfected cells ($n = 5$, $^{**}p < 0.01$) were statistically significant. *B*, The amplitude of the first spike. The amplitude was larger in mKv4.2dn-transfected cells and smaller in mKv4.2-transfected cells compared with control cells. Mean ± SEM. The differences between control cells and mKv4.2dn-transfected cells, or between control cells and mKv4.2-transfected cells were statistically significant ($^*p < 0.05$). *C–E*, The threshold of action potential (*C*), amplitude of AHP (*D*), and RMP (*E*) did not appear to be affected by changes in A-type current properties.

A potassium channel blocker 4-AP is commonly used to analyze the role of current components. When the functional role of I_A in action potential in the cerebellar granule cells was studied by blocking I_A with 1 mM 4-AP, not only the first spike latency but also afterhyperpolarization and frequency of spikes were affected drastically (D'Angelo et al., 1998). Such multiple effects on the discharge pattern were thought to be caused by partial inhibition of tetraethylammonium-sensitive delayed rectifier components (Belluzzi et al., 1985; Numann et al., 1987; Cull-Candy et al., 1989; Wang et al., 1991; Bardoni and Belluzzi, 1993). Our experiments using the dominant-negative constructs illustrate the role of genuine I_A encoded by Kv4 subunits.

The various parameters of I_A, such as activation, inactivation, and recovery from inactivation (see Figs. 4, 5), aptly account for the observed discharge characteristics. First, because the RMP of mature T-shaped cells was near −80 mV, A-type channels could be fully activated when the cells were depolarized. Second, I_A should be inactivated after the first spike and recover from inactivation by an AHP at a potential more negative than −50 mV (Fig. 5). These characteristics of I_A cause the limited effect on regulation of action potential. It should be noted, however, that the voltage dependency of activation and inactivation of I_A we observed displayed more positive potential compared with that observed in other cells and the cerebellar granule cells in different experimental conditions (Bardoni and Belluzzi, 1993; Serodio et al., 1994). The differences of voltage dependency might be explained by different modifications of channel proteins or subunit composition.

A similar effect of fast-inactivating K^+ current on excitability was reported using pyramidal neurons in dorsal cochlear nuclei

(Kanold and Manis, 1999). In these cells, the latency before the generation of the first spike of action potential decreased as the membrane potential became more positive, whereupon only the fast-inactivating K^+ current (I_{K1F}) should inactivate before depolarizing stimulation. These cells maintained their repetitive discharge in this condition. This result strongly supports our conclusion that I_A produced by Kv4 channels primarily participates in suppression of the first spike. However, it should also be noted that the amplitude of AHP observed in our microexplant culture was smaller (approximately −50 mV) (Fig. 10*D*) than that observed in granule cells *in vivo* at approximately postnatal day 20 (P20) (approximately −80 mV) (D'Angelo et al., 1997, 1998). Therefore, the effect of the K^+ current under the AHP near −80 mV remains to be investigated.

Our results demonstrated that the majority of the I_A was conducted by the Kv4 family; however, the current could not be eliminated completely by the expression of mKv4.2dn (Fig. 7*C*), and ~25% of the peak current remained. This suggests several possibilities: first, the turnover rate of the functional Kv4 channel complex was too slow to be replaced during our experiments using the transient expression system; second, the expression level of mKv4.2dn was insufficient; or third, channels other than Kv4 were involved in the I_A. It has been reported that Kv1.1 in combination with Kvβ1 β-subunit encodes A-type channels when expressed in *Xenopus* oocytes (Rettig et al., 1994; Heinemann et al., 1996; Sewing et al., 1996). Our *in situ* hybridization experiments *in vivo* showed that the Kv1.1 mRNA could be detected in the internal granule layer (IGL) at the second postnatal week (data not shown), suggesting that this channel might contribute to the I_A. The Kvβ1 subunit is also known to be expressed in external granule layer and IGL at early postnatal stages (Downen et al., 1999). We did not examine the expression of the Kv1.1 gene in the microexplant culture, but these results suggest that Kv1.1 may be expressed at low levels in our system and give rise to the residual I_A after the elimination by mKv4.2dn.

Expression system as a tool for channel analysis

When expressed in an heterologous expression system, cloned mKv4.2 currents differ significantly from native I_A in a number of properties, such as inactivation rate and 4-AP sensitivity (Serodio et al., 1994, 1996). For example, the cloned homomeric Kv4.2 current expressed in *Xenopus* oocytes exhibited half-activation at 0 mV and half-inactivation at −60 mV, with two voltage-dependent inactivation constants of 20–40 and 100–200 msec. On the other hand, in the cerebellar granule cells, I_A displayed half-activation at −46.7 mV and half-inactivation at −78.8 mV, with one voltage-independent inactivation constant of 19 msec (Bardoni and Belluzzi, 1993). In this study, the mKv4.2 current expressed in HEK293 cells and the I_A in mouse cerebellar granule cells also exhibited different inactivation constants (Figs. 6, 8). In most cases, β-subunits accelerate the inactivation rate of functional α-subunit channels (Rettig et al., 1994; Heinemann et al., 1996; Sewing et al., 1996). Furthermore, intracellular modulation of the channels, such as phosphorylation, also alters the kinetics of channel gating. It is plausible that differences of channel properties observed between *in vivo* and *in vitro* systems are attributable to these factors.

One of the interesting findings in our results is that the inactivation rate of I_A became very similar to that of the mKv4.2 current in HEK293 cells when wild-type mKv4.2 was introduced into the granule cells (Fig. 8). Although the experiment was designed to overcome the limitations of the heterologous expression system, the outcome appears to indicate that the introduced gene overrides the intrinsic system. This change in kinetics of native I_A may be explained by several possibilities: (1) excess wild-type mKv4.2 expression may result in the formation of unusual homomultimers that exclude Kv4.3 involved in native complex formation; (2) intrinsic Kv4.2 channels in granule cells are different isoforms from cloned mKv4.2; and (3) extrinsic mKv4.2 failed to be processed properly by cellular modification mechanisms. It also should be noted that transfection of equal amounts of mKv4.2 cDNA and EGFP cDNA causes serious damage to the granule cells (over 10 cells per explant survived when EGFP or EGFP plus mKv4.2dn were transfected, whereas only 1–2 cells per explant survived when mKv4.2 were transfected in addition to EGFP). Because this cell death could not be rescued by the application of 1 μM TTX or 2 mM 4-AP in the culture medium to block channel activity, the toxic effect might not be mediated by the regular channel function on the cell surface. It may instead be caused by abnormal accumulation of mKv4.2 in the Golgi apparatus or in some other organelles.

Developmental role of I_A encoded by the Kv4 subfamily

In general, I_A is thought to function in dendrites and synapses to regulate the excitability of the postsynaptic membrane and hence control the reception and integration of synaptic signals in the adult brain (Sheng et al., 1992; Hoffman et al., 1997). Previously, we reported (Shibata et al., 1999) that Kv4.2 immunoreactivity was detectable in the glomeruli of IGL in adult mice, whereas at P7 it is detected in the cell body of granule cells in the PMZ and IGL. Kv4.2 proteins were also localized in the cell body of granule cells in microexplant cultures. Our results suggest that I_A encoded by the Kv4 family functions in the cell body and regulates electrical excitability to determine the differentiation of granule cells in a manner distinct from that in the postsynapse. Cell migration and morphological change, however, were not affected by the elimination or overexpression of I_A (data not shown). The influences of I_A on neuronal development remain to be examined.

REFERENCES

Arhem P, Johansson S (1989) A model for the fast 4-aminopyridine effects on amphibian myelinated nerve fibres. A study based on voltage-clamp experiments. Acta Physiol Scand 137:53–61.

Baldwin TJ, Tsaur ML, Lopez GA, Jan YN, Jan LY (1991) Characterization of a mammalian cDNA for an inactivating voltage-sensitive K^+ channel. Neuron 7:471–483.

Bardoni R, Belluzzi O (1993) Kinetic study and numerical reconstruction of A-type current in granule cells of rat cerebellar slices. J Neurophysiol 69:2222–2231.

Belluzzi O, Sacchi O, Wanke E (1985) A fast transient outward current in the rat sympathetic neurone studied under voltage-clamp conditions. J Physiol (Lond) 358:91–108.

Campbell DL, Qu Y, Rasmusson RL, Strauss HC (1993) The calcium-independent transient outward potassium current in isolated ferret right ventricular myocytes. II. Closed state reverse use-dependent block by 4-aminopyridine. J Gen Physiol 101:603–626.

Castle NA, Slawsky MT (1993) Characterization of 4-aminopyridine block of the transient outward K^+ current in adult rat ventricular myocytes. J Pharmacol Exp Ther 265:1450–1459.

Choquet D, Korn H (1992) Mechanism of 4-aminopyridine action on voltage-gated potassium channels in lymphocytes. J Gen Physiol 99:217–240.

Cull-Candy SG, Marshall CG, Ogden D (1989) Voltage-activated membrane currents in rat cerebellar granule neurones. J Physiol (Lond) 414:179–199.

D'Angelo E, De Filippi G, Rossi P, Taglietti V (1997) Synaptic activation of Ca^{2+} action potentials in immature rat cerebellar granule cells *in situ*. J Neurophysiol 78:1631–1642.

D'Angelo E, De Filippi G, Rossi P, Taglietti V (1998) Ionic mechanism

of electroresponsiveness in cerebellar granule cells implicates the action of a persistent sodium current. J Neurophysiol 80:493–503.
Davies NW, Pettit AI, Agarwal R, Standen NB (1991) The flickery block of ATP-dependent potassium channels of skeletal muscle by internal 4-aminopyridine. Pflügers Arch 419:25–31.
Downen M, Belkowski S, Knowles H, Cardillo M, Prystowsky MB (1999) Developmental expression of voltage-gated potassium channel β subunits. Brain Res Dev Brain Res 117:71–80.
Fisher TE, Voisin DL, Bourque CW (1998) Density of transient K^+ current influences excitability in acutely isolated vasopressin and oxytocin neurones of rat hypothalamus. J Physiol (Lond) 511:423–432.
Gorter JA, Aronica E, Hack NJ, Balazs R, Wadman WJ (1995) Development of voltage-activated potassium currents in cultured cerebellar granule neurons under different growth conditions. J Neurophysiol 74:298–306.
Heinemann SH, Rettig J, Graack HR, Pongs O (1996) Functional characterization of Kv channel β-subunits from rat brain. J Physiol (Lond) 493:625–633.
Hoffman DA, Johnston D (1998) Downregulation of transient K^+ channels in dendrites of hippocampal CA1 pyramidal neurons by activation of PKA and PKC. J Neurosci 18:3521–3528.
Hoffman DA, Magee JC, Colbert CM, Johnston D (1997) K^+ channel regulation of signal propagation in dendrites of hippocampal pyramidal neurons. Nature 387:869–875.
Johns DC, Nuss HB, Marban E (1997) Suppression of neuronal and cardiac transient outward currents by viral gene transfer of dominant-negative Kv4.2 constructs. J Biol Chem 272:31598–31603.
Kanold PO, Manis PB (1999) Transient potassium currents regulate the discharge patterns of dorsal cochlear nucleus pyramidal cells. J Neurosci 19:2195–2208.
Kehl SJ (1990) 4-Aminopyridine causes a voltage-dependent block of the transient outward K^+ current in rat melanotrophs. J Physiol (Lond) 431:515–528.
Keros S, McBain CJ (1997) Arachidonic acid inhibits transient potassium currents and broadens action potentials during electrographic seizures in hippocampal pyramidal and inhibitory interneurons. J Neurosci 17:3476–3487.
Martina M, Schultz JH, Ehmke H, Monyer H, Jonas P (1998) Functional and molecular differences between voltage-gated K^+ channels of fast-spiking interneurons and pyramidal neurons of rat hippocampus. J Neurosci 18:8111–8125.
Nagata I, Nakatsuji N (1990) Granule cell behavior on laminin in cerebellar microexplant cultures. Brain Res Dev Brain Res 52:63–73.
Numann RE, Wadman WJ, Wong RK (1987) Outward currents of single hippocampal cells obtained from the adult guinea-pig. J Physiol (Lond) 393:331–353.
Ramoa AS, McCormick DA (1994) Developmental changes in electrophysiological properties of LGNd neurons during reorganization of retinogeniculate connections. J Neurosci 14:2089–2097.
Rettig J, Heinemann SH, Wunder F, Lorra C, Parcej DN, Dolly JO, Pongs O (1994) Inactivation properties of voltage-gated K^+ channels altered by presence of β-subunit. Nature 369:289–294.
Rogawski MA, Beinfeld MC, Hays SE, Hokfelt T, Skirboll LR (1985) Cholecystokinin and cultured spinal neurons. Immunohistochemistry, receptor binding, and neurophysiology. Ann NY Acad Sci 448:403–412.
Rossi P, De Filippi G, Armano S, Taglietti V, D'Angelo E (1998) The weaver mutation causes a loss of inward rectifier current regulation in premigratory granule cells of the mouse cerebellum. J Neurosci 18:3537–3547.
Rudy B, Hoger JH, Lester HA, Davidson N (1988) At least two mRNA species contribute to the properties of rat brain A-type potassium channels expressed in *Xenopus* oocytes. Neuron 1:649–658.
Schroter KH, Ruppersberg JP, Wunder F, Rettig J, Stocker M, Pongs O (1991) Cloning and functional expression of a TEA-sensitive A-type potassium channel from rat brain. FEBS Lett 278:211–216.
Serodio P, Rudy B (1998) Differential expression of Kv4 K^+ channel subunits mediating subthreshold transient K^+ (A-type) currents in rat brain. J Neurophysiol 79:1081–1091.
Serodio P, Kentros C, Rudy B (1994) Identification of molecular components of A-type channels activating at subthreshold potentials. J Neurophysiol 72:1516–1529.
Serodio P, Vega-Saenz de Miera E, Rudy B (1996) Cloning of a novel component of A-type K^+ channels operating at subthreshold potentials with unique expression in heart and brain. J Neurophysiol 75:2174–2179.
Sewing S, Roeper J, Pongs O (1996) Kv β1 subunit binding specific for shaker-related potassium channel α subunits. Neuron 16:455–463.
Sheng M, Tsaur ML, Jan YN, Jan LY (1992) Subcellular segregation of two A-type K^+ channel proteins in rat central neurons. Neuron 9:271–284.
Shibata R, Wakazono Y, Nakahira K, Trimmer JS, Ikenaka K (1999) Expression of Kv3.1 and Kv4.2 genes in developing cerebellar granule cells. Dev Neurosci 21:87–93.
Song WJ, Tkatch T, Baranauskas G, Ichinohe N, Kitai ST, Surmeier DJ (1998) Somatodendritic depolarization-activated potassium currents in rat neostriatal cholinergic interneurons are predominantly of the A type and attributable to coexpression of Kv4.2 and Kv4.1 subunits. J Neurosci 18:3124–3137.
Spitzer NC (1995) Spontaneous activity: functions of calcium transients in neuronal differentiation. Perspect Dev Neurobiol 2:379–386.
Surmeier DJ, Mermelstein PG, Goldowitz D (1996) The weaver mutation of GIRK2 results in a loss of inwardly rectifying K^+ current in cerebellar granule cells. Proc Natl Acad Sci USA 93:11191–11195.
Thompson S (1982) Aminopyridine block of transient potassium current. J Gen Physiol 80:1–18.
Tsaur ML, Chou CC, Shih YH, Wang HL (1997) Cloning, expression and CNS distribution of Kv4.3, an A-type K^+ channel α subunit. FEBS Lett 400:215–220.
Wakazono Y, Kurahashi T, Nakahira K, Nagata I, Takayama C, Inoue Y, Kaneko A, Ikenaka K (1997) Appearance of a fast inactivating voltage-dependent K^+ currents in developing cerebellar granule cells *in vitro*. Neurosci Res 29:291–301.
Wang Y, Strahlendorf JC, Strahlendorf HK (1991) A transient voltage-dependent outward potassium current in mammalian cerebellar Purkinje cells. Brain Res 567:153–158.
Yeh JZ, Oxford GS, Wu CH, Narahashi T (1976) Dynamics of aminopyridine block of potassium channels in squid axon membrane. J Gen Physiol 68:519–535.